

Towards a PAT-Based Strategy for Crystallization Development

Melissa Birch, Steven J. Fussell, Paul D. Higginson, Neil McDowall, and Ivan Marziano*

Pfizer Global Research and Development, Ramsgate Road, Sandwich CT13 9NJ, United Kingdom

Abstract:

A strategy for the rapid, material-efficient development of crystallization processes centred around the use of process analytical technology (PAT) is presented and demonstrated on an active pharmaceutical ingredient (API) currently in development at Pfizer's Sandwich laboratories. PAT is implemented at scales as small as 1 mL in high-throughput equipment, enabling the early acquisition of key data to select the best crystallization approach. At a larger scale, PAT offers a window into process kinetics and, for the case study discussed in this contribution, highlighted vulnerabilities of the process arising from the formation of a labile solvate. A combination of on-line and off-line analyses provided the basis for a full assessment of the process.

Introduction

The application of process analytical technology (PAT) to crystallization is currently an area of high interest for both the chemical development and manufacturing arenas. This scenario is partly due to the growing emphasis on PAT as a tool for "21st Century Manufacturing" as described, for example, in the guideline document "PAT -- A Framework for Innovative Pharmaceutical Development, Manufacturing, and Quality Assurance" issued by the U.S. Food and Drug Administration (FDA) in 2004.¹ This effort, however, is also a reflection of the increasing awareness within the chemical industry that crystallization processes are often poorly understood and poorly controlled. In this context, PAT is a key tool for mechanistic elucidation and for the assessment of causes and extent of process deviations on scale-up or transfer to a different facility. Crucially, any effort in this direction must be associated with a molecular understanding of crystal properties, for example with regards to polymorphism and solvent-solute interactions.²

Applications of PAT to crystallization processes have been recently reviewed³ and can be broadly classified in four categories:

(1) the use of on-line sensors (primarily FT-IR spectroscopy) to monitor and control solution concentration throughout the crystallization. Berglund⁴ first proposed and demonstrated the applicability of ATR-FT-IR spectroscopy for monitoring solution concentration in the early 1990s. Wide-

spread interest from Industry and Academia has resulted in a number of subsequent publications providing additional examples of application for the control of crystallization processes⁵⁻⁸

(2) the use of PAT (typically Raman or near-IR spectroscopy) to monitor polymorph or pseudopolymorph conversion in real time, with a view to understand the kinetics of the transition and gain the knowledge necessary to develop a robust process⁹⁻¹¹

(3) applications to a control strategy based on first principles as described, for example, by Braatz¹²

(4) particle engineering through monitoring and control of the crystal size distribution via a PAT tool, most commonly focused beam reflectance measurements (FBRM).^{13,14}

In this contribution, a PAT-based approach for the development of crystallization processes for active pharmaceutical ingredients (APIs) is presented. The necessity for developing a strategy stems from a desire to initiate a structured program at the interface between the discovery and development of APIs. Here PAT is used for measurement and understanding, rather than as release test or control tool. Initial efforts concentrate on selecting an appropriate solvent for a reactive step (where applicable) and product isolation using high-throughput methodology.¹⁵ The most promising hits are then evaluated further by building solubility and metastable zone edge curves effectively by carrying out PAT measurements at the 1-mL scale. If this is sufficient to identify suitable crystallization conditions, a process is defined and carried out at the 40-mL scale, where information on the kinetics can be gained, for example, through FBRM and Raman spectroscopy. The next step would be to explore process parameters using statistical design of experiments (DoE) to assess robustness and opportunities for further optimization.¹⁶ Transfer to scale-up facilities, where PAT is also applied, can offer opportunities for further assessing the

* To whom correspondence should be addressed. E-mail: ivan.marziano@pfizer.com.

(1) FDA guidelines on PAT: <http://www.fda.gov/cder/guidance/6419fnl.htm>.
(2) Davey, R. J. *Chem. Commun.* **2003**, 23, 1463.
(3) Yu, L. X.; Lionberger, R. A.; Raw, A. S.; D'Costa, R.; Wu, H.; Hussain, A. S. *Adv. Drug Delivery Rev.* **2004**, 56, 349.
(4) Dunuwila, D. D.; Carroll, L. B.; Berglund, K. A. *J. Cryst. Growth* **1994**, 137, 561.

(5) Groen, H.; Borissova, A.; Roberts, K. *J. Ind. Eng. Chem. Res.* **2003**, 42, 198.
(6) Fevotte, G. *Int. J. Pharm.* **2002**, 241, 263.
(7) Togkalidou, T.; Fujiwara, M.; Patel, S.; Braatz, R. D. *J. Cryst. Growth* **2001**, 231, 534.
(8) Liotta, V.; Sabesan, V. *Org. Process Res. Dev.* **2004**, 8, 488.
(9) Norris, T.; Aldridge, P. K.; Sekulic, S. S. *Analyst* **1997**, 122, 549.
(10) Starbuck, C.; Spartalis, A.; Wai, L.; Wang, J.; Fernandez, P.; Lindemann, C. M.; Zhou, G. X.; Ge, Z. *Cryst. Growth. Des.* **2002**, 2, 515.
(11) Hussmann, G. A.; Berglund, K. A.; Larson, M. A. *Appl. Spectrosc.* **1985**, 39, 560.
(12) Togkalidou, T.; Tung, H.; Sun, Y.; Andrews, A. T.; Braatz, R. D. *Ind. Eng. Chem. Res.* **2004**, 43, 6168.
(13) FBRM is a Lasentec/Mettler Toledo product. Details on <http://www.lasentec.com>.
(14) Barrett, P.; Glennon, B. *Part. Part. Syst. Charact.* **1999**, 16, 207.
(15) Higginson, P. D.; Sach, N. W. *Org. Process Res. Dev.* **2004**, 8, 1009.
(16) Togkalidou, T.; Braatz, R. D.; Johnson, B. K.; Davidson, O.; Andrews, A. *AIChE J.* **2001**, 47, 160.

Table 1. Solubility^a of compound A (in g/L of solvent) in various solvents at room temperature and 50 °C

solvent	solubility (g/L)		solvent	solubility (g/L)	
	rt	50 °C		rt	50 °C
methanol	18	25	<i>n</i> -amyl alcohol	19	22
acetonitrile	10	11	2-methyl-2-butanol	7	12
ethanol	22	–	dichloromethane	33	117
acetone	56	74	DMF	>200	>200
acetic acid	43	52	DMSO	>200	>200
<i>n</i> -propanol	13	34	trifluorotoluene	6	–
2-propanol	21	–	octanol	17	–
<i>n</i> -butanol	19	–	cyclopentanol	21	27
<i>i</i> -butyl alcohol	16	25	methanol/water, 90:10 v/v	28	–
<i>s</i> -butyl alcohol	5	–	methanol/acetone, 50:50 v/v	37	47
<i>tert</i> -butyl alcohol	14	11	acetonitrile/water, 90:10 v/v	16	16
MEK	31	77	acetonitrile/acetone, 50:50 v/v	16	35
THF	66	120	ethanol/water, 90:10 v/v	23	20
MeOAc	17	–	ethanol/acetone, 50:50 v/v	–	43
EtOAc	9	22	acetone/water, 90:10 v/v	28	54
<i>n</i> -PrOAc	14	29	2-propanol/water, 90:10 v/v	22	27
<i>i</i> -PrOAc	7	26	2-propanol/acetone, 50:50 v/v	26	–
MEK/water, 90:10 v/v	33	70	THF/water, 90:10 v/v	100	146
MEK/acetone, 50:50 v/v	40	81	THF/acetone, 50:50 v/v	–	146

^a Missing data points refer to mixtures for which the clear supernatant liquid could not be obtained.

validity of laboratory models and refining them as appropriate.

The application of this strategy is illustrated on a current API, compound A, with the objective of introducing process understanding early on in development, and to introduce a data-driven decision-making approach based on a combination of scientific facts and practical considerations.

Experimental Section

(i) Solubility Screen. A representative selection of viable solvents was selected, taking into account previous experience with compound A, but also low toxicity and physical diversity, e.g. in terms of dielectric constants. The Powdernium Autodose was used to dispense a known amount of compound A to 1-mL vials. Laboratory-grade solvents and compound A of representative quality were used. The ReactArray SK233 Workstation was then used to dispense the relevant solvents to produce slurried samples. After magnetic stirring for several hours to ensure saturation at room temperature, a known volume of the clear supernatant was removed and analysed gravimetrically post removal of solvent in vacuo. The original slurry samples were then resealed, held at 50 °C and sampled as before.

(ii) One-Milliliter-Solubility/Metastable Zone Edge Curves Determination. The Avantium Crystal16 platform (formerly known as the MiniMax) is composed of 16 wells designed to hold 1-mL vials, each with its own on-line turbidity sensor. The wells can be magnetically stirred at a fixed speed and are grouped into four zones that can be independently heated and cooled. Slurries of compound A in each of the four candidate solvents (selected from the previous screen to accommodate the platform's capabilities in terms of independent heating) were prepared to four concentrations. The Crystal16 heated and cooled these slurries at 0.3 °C/min from 20 °C to reflux and back to 20 °C. To increase the confidence in the results, this heat/cool

cycle was repeated a further two times. Lower concentration measurements were performed after crash-cooling solutions of compound A.

(iii) Forty-Milliliter-Scale Experiments. Experiments at 40-mL scale were performed on the Mettler Toledo Multi-Max IR platform. Compound A was dissolved in methyl ethyl ketone (MEK)/water 91:9 v/v at reflux. The stirred solution was then cooled at 0.3 °C/min to 0 °C, where the mixture was held over 16 h. Two experiments were performed, the first using on-line Raman (Kaiser HoloLab series 5000), followed by ¹H NMR spectroscopy, microscopy, and HPLC analysis to assess viability; the second experiment employed FBRM (Mettler Toledo Lasentec D600L), Raman, and IR on-line analysis in conjunction with off-line analysis. Yields of 83–85% were recorded. Raman spectral data were analysed by Infometrix Pirouette software.

Results and Discussion

(i) Solubility Screen. An initial solubility screen was performed on compound A, using 38 solvents and binary solvent mixtures. The results are listed in Table 1. Ideally, a solvent allowing a cooling crystallization should be identified, as these processes are easier to scale-up than, for example, anti-solvent crystallizations, where differences in micro- and macro-mixing at the larger scale could deliver unexpected results. As well as not presenting any stability issues in combination with the API, a desirable solvent for the cooling crystallization of pharmaceutical compounds should display a number of characteristics:

- sufficient dependence of the solubility on the temperature to ensure acceptable yield whilst minimizing the amount of solvent used
- the presence of a temperature window between reflux and the dissolution point at the working concentration to ensure robust filtration of particulate matters (speck-freeing filtration)

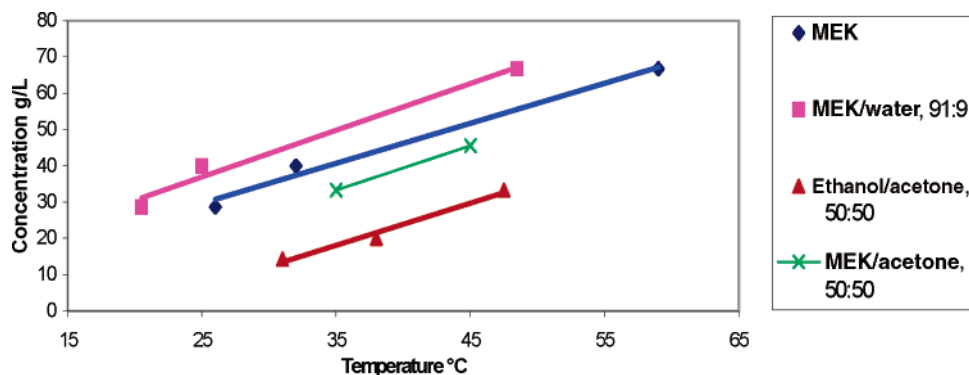


Figure 1. Solubility measurements for compound A in MEK, MEK/water (91:9 v/v), EtOH/acetone (50:50 v/v), and MEK/acetone (50:50 v/v).

- the ability to deliver the API in the desired solid form
- residual solvent levels in the API must be compatible with ICH guidelines¹⁷
- the potential to remove impurities due to differential solubility – where applicable
- a metastable zone width sufficient to enable robust seeding – where applicable
- ease of solvent recovery (e.g. through azeotropic distillations)
- low environmental impact.

(ii) One-Milliliter-Solubility/Metastable Zone Edge Curves Determination. The application of these criteria led to the identification of four potential solvent systems out of those screened (Table 1): methyl ethyl ketone (MEK), MEK/water (91:9 v/v), ethanol/acetone (50:50 v/v, also identified as potential during previous experiments), MEK/acetone (50:50 v/v). Basic solubility curves on these solvent systems were measured using the Avantium Crystal16 (Figure 1), and showed that the most promising system was MEK/water, based on the criteria listed above. The 91:9 v/v MEK/water ratio was used instead of the 90:10 v/v ratio adopted during solubility tests due to operator error. The values shown in Figure 1 are slightly different from those reported in Table 1 due to the different techniques used.

Following these results, efforts were concentrated first on identifying the optimum MEK/water ratio, confirmed as MEK/water 91:9 v/v using the Crystal16 system, which provided the best combination of dissolution temperature and recovery yield. Further efforts were invested in measuring solubility and metastable zone edge curves for this solvent mixture. A typical experiment would consist of preparing a slurry of a known amount of solid in 1 mL of the solvent mixture, heating to 75 °C at 0.3 °C/min (magnetic stir bars are used for agitation) and cooling at 0.3 °C/min to 0 °C to observe the dissolution temperature and the onset of crystallization by turbidity. Each measurement cycle was repeated twice to increase confidence in the results. The use of magnetic stir bars in 1-mL vials will result in narrow metastable zone widths compared to larger scale, overhead-agitated vessels, due to the contact between the agitation medium and the vessel. This represents a “worst-case scenario”, providing a higher level of confidence that

uncontrolled nucleation events will be avoided at a larger scale.

This set of measurement yielded unexpected results. While a solubility curve could be easily built using data from the first cycle of each measurement, at the lower concentrations the dissolution temperature was much lower for the second and third cycles than it was for the first. This was interpreted as symptomatic of the formation of a polymorph or pseudopolymorph, and indeed an earlier screen carried out by colleagues in Material Sciences had highlighted the formation of a labile MEK solvate for compound A. The solvate is unstable upon removal from the solvent medium. The data (Figure 2) also show that the desired anhydrous form is more stable than the solvate (as indicated by its lower solubility) at higher temperatures, and stable to MEK, i.e. the anhydrous form will not convert to the solvate in the presence of MEK within the time scale of the experiment, but a recrystallization is necessary to obtain the solvate. Using data from the Crystal16, solubility and metastable edge curves for both solid forms were obtained. These data are acquired using a more robust protocol than the data shown in Figure 1; hence, values of solubility can differ slightly.

Further information can be gathered from the data presented in Figure 2. Assuming that a 15 °C temperature drop is observed during speck-free filtration, the equilibrium solubility at 58 °C (which is 15 °C below the boiling point of the MEK/water azeotrope) is approximately 88 g/L or 11.4 mL/g. This is based on the solubility of the desired anhydrous form and represents the maximum concentration for this process if speck-freeing is required.

The expected yield from an isolation at 0 °C is 93% and could be improved further by azeotropic distillation post speck-freeing. On the basis of the lower entropy of a slurry of solvate crystals compared to that of a slurry of anhydrous crystals, the solvate would be expected to gain stability at lower temperatures and could potentially become the more stable form within the temperature range of the crystallization process. The data presented in Figure 2 confirm that, at this MEK/water ratio, at temperatures lower than ca. 14 °C the solvate would be the thermodynamically more stable form, as highlighted by its lower solubility. Correspondingly, even if the anhydrous form crystallizes first at a higher temperature, a conversion may eventually take place to the MEK solvate. Information available from previous experiments

(17) ICH guidelines on residual solvent levels are available from <http://www.ich.org>.

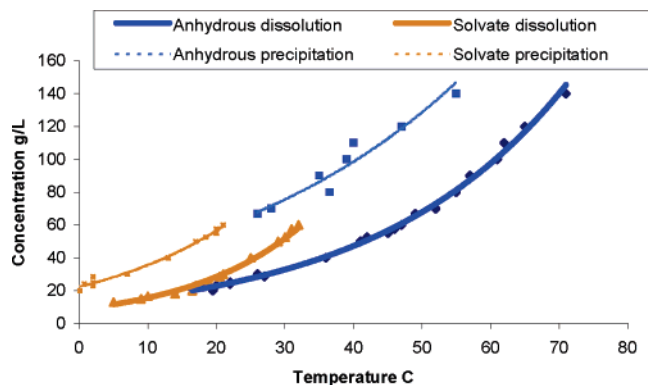


Figure 2. Solubility and metastable zone edge curves for postulated anhydrous and solvate forms of compound A in MEK/water 91:9 v/v. The y axis is g of compound A in L of solvent mixture.

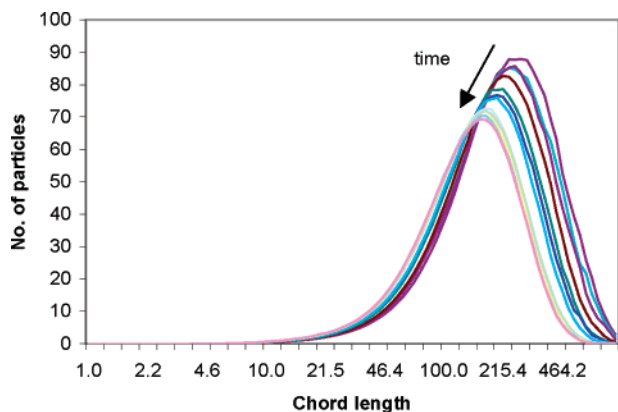


Figure 3. Chord length distributions at various time points. Chord length in μm is plotted on the x-axis, number of particles on the y-axis. The first timepoint corresponds to 40 min after the start of crystallization, the last to the endpoint.

suggests that an MEK solvate would be labile, and the expectation is for the MEK solvate to be converted to anhydrous form during filtration/drying, but this may impair the quality of the resulting crystals if the solvent is an integral part of the crystal lattice.

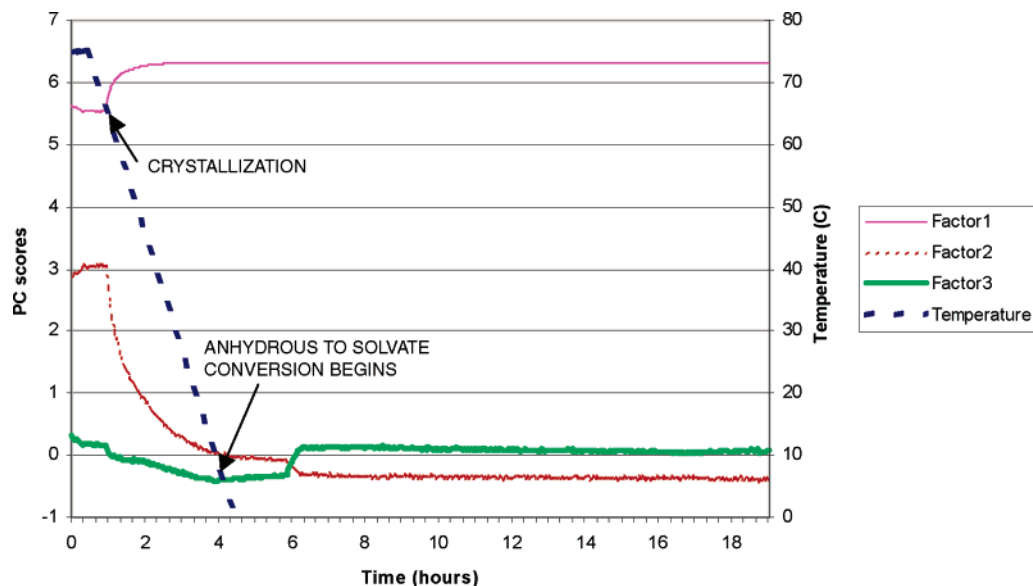


Figure 4. Plot of reactor temperature and first three principal component scores from Raman spectral data for a 40-mL crystallization experiment.

(iii) Forty-Milliliter-Scale Experiments. The viability of an MEK/water process was initially confirmed by a single experiment at 40-mL scale. A yield of 85% was obtained from this experiment. ^1H NMR showed a negligible amount of MEK in the isolated solid. Microscopy showed that small crystals (around $5\ \mu\text{m}$ in size) were formed, and HPLC demonstrated that an increase in purity was observed, with the removal of a single impurity quantified at 1.5% w/w in the starting material. No seeding was used for this experiment.

A further experiment was performed where seeding was carried out at $64\ ^\circ\text{C}$, which is between one-third and one-half the metastable zone width, closer to the solubility line.¹⁸ This crystallization was monitored by Raman spectroscopy and by FBRM, to understand process kinetics in terms of nucleation, growth, and form conversion events. At an isolation temperature of $3\ ^\circ\text{C}$, the solvate was expected to be the most stable form; hence, a conversion of the initially precipitated anhydrous form to the MEK solvate could be anticipated. A change in chord length distribution as measured by FBRM, Figure 3, was observed throughout the process. The data show that following the initial crystallization event a continuous downward shift in chord length is observed, perhaps symptomatic of a form change.

Alongside the main crystallization event, a principal component analysis of the Raman spectral data shows a second event, which was attributed to the form conversion and shows the expected sigmoidal profile (Figure 4).⁸ This type of profile is associated with the presence of three separate processes: dissolution of the metastable form, nucleation of the stable form, and growth of the stable form. The three processes take place at different rates and, hence, the sigmoidal rate profile. The data show that, at this MEK/water ratio and during cooling to $3\ ^\circ\text{C}$, the anhydrous form converts into the MEK solvate within 2.5 h. The temperature at which the incipient form conversion (ca. $11\ ^\circ\text{C}$) is observed is somewhat lower than that predicted (ca. $14\ ^\circ\text{C}$), probably due to a kinetic effect.

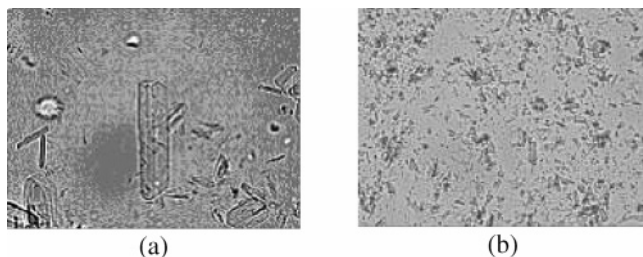


Figure 5. Comparison of prefiltration (a) and postdrying material (b) by microscopy to show the change in particle size and shape. Each image is $155\ \mu\text{m} \times 115\ \mu\text{m}$, with a $\times 40$ magnification.

The observation that the crystals obtained from the unseeded and seeded processes were essentially of the same size (ca. $5\ \mu\text{m}$) suggests that the desolvation event leads to a partial collapse of the crystal lattice, resulting in the formation of small particles. To confirm this theory, recrystallized material was analysed by microscopy prefiltering and postdrying. Analysis of the prefiltration slurry showed that crystals typically measured $40\ \mu\text{m}$, whereas crystals obtained postdrying show a typical particle size of $5\ \mu\text{m}$ (Figure 5). This comparison confirms that the solvation/desolvation process has a profound impact on the crystal lattice and, hence on the particle size distribution. This behaviour indicates that the solvent is an integral part of the crystal lattice, whereas for other compounds the solvent may be easily removed without causing a major structural disruption.

Conclusions

The application of a strategy to the development of crystallization processes based on high throughput systems and PAT was exemplified on an API. The strengths of this methodology consist of: (i) identification of best solvent media through high throughput solubility screens, (ii) identification of best approach to crystallization via small-scale PAT, (iii) understanding the properties of the solid/solvent system through PAT.

(18) Beckmann, W. *Org. Process Res. Dev.* **2000**, *4*, 372.

The results highlighted the need to assess polymorphism, hydration, and solvation properties of the solid throughout the process development period to understand the observed behaviour. Data relating to compound A showed that desolvation of an MEK solvate can result in the formation of small particles and that this process is unsuitable for engineering particle size through the crystallization. Not all of these occurrences were highlighted by PAT (e.g. solvate collapse on drying), underlining the key point that PAT is not a substitute for traditional characterization techniques but provides an in situ tool for understanding. Three scenarios are possible at this point:

- The solid obtained for this process does not pose a problem during downstream processing and formulation; hence, this crystallization approach is viable.
- The solid is isolated at a higher temperature, e.g., $25\ ^\circ\text{C}$, to avoid solvation, although an 8% yield reduction would be anticipated.
- A new solvent system is identified which does not give rise to solvate formation.

Throughout this study, the application of PAT has consistently delivered a unique insight into the properties of the process, ultimately enabling the rapid identification of a crystallization protocol and its possible downfalls. Further plans involve scale-up of the process to enable formulation studies and understand whether material obtained via this route is viable. PAT will also be used during scale-up to gain further insight on process kinetics and robustness.

Acknowledgment

We thank Katie Wilford of Pfizer Global Research and Development for experimental assistance, Catherine Dunne, Neil Feeder, and Alistair Swanson of Pfizer Global Research and Development for useful discussions, and Arjen van Langevelde, Danny Stam, and Guus Scheefhals of Avantium for technical assistance. The reviewers are also thanked for helpful suggestions.

Received for review January 14, 2005.

OP0500077